FEBS Letters 587 (2013) 2420–2429

journal homepage: www.FEBSLetters.org

ATF4 activation by the p38MAPK–eIF4E axis mediates apoptosis and autophagy induced by selenite in Jurkat cells

Qian Jiang, Feng Li, Kejian Shi, Pa Wu, Jiajia An, Yang Yang, Caimin Xu *

National Laboratory of Medical Molecular Biology, Institute of Basic Medicine Sciences & School of Basic Medicine, Peking Union Medical College and Chinese Academy of Medical Sciences, Beijing 100005, China

ARTICLE INFO

Article history:
Received 8 March 2013
Revised 5 June 2013
Accepted 5 June 2013
Available online 19 June 2013

Edited by Angel Nebreda

Keywords:
Sodium selenite
p38MAPK
Apoptosis
Autophagy
eIF4E
ATF4

ABSTRACT

Previous studies have shown that selenite exerts pro-apoptosis and pro-autophagy effects and is associated with the activation of ER stress in T-cell acute lymphoblastic leukemia (T-ALL). Herein we demonstrate the underlying mechanisms by which the activation of p38MAPK plays essential roles in apoptosis and autophagy and the coordination of cellular metabolic processes during leukemia therapy. MKK3/6-dependent activation of p38MAPK is required for the phosphorylation of eIF4E, thus initiating the translation of ER stress-related transcription factor ATF4. Upregulated ATF4 results in the transcriptional initiation of the apoptosis-related *chop* gene and autophagy-related *map1lc3b* gene, through which selenite links ER stress to apoptosis and autophagy during leukemia treatment. Moreover, autophagy induction enhances cell apoptosis under this condition.

1. Introduction

T-cell acute lymphoblastic leukemia (T-ALL) is an aggressive and heterogeneous disease characterized by an abnormal increase in immature white blood cells [1,2]. Chemotherapy is the main strategy used to treat leukemia, whereas the major obstacle to treatment is the resistance of leukemic cells to various chemotherapeutic agents [3,4]. Our previous findings document effective antitumor efficacy of sodium selenite in leukemia by eliciting ER stress-related apoptosis or autophagy [5,6]. However, the conversation among them was still not clear. Hence, a detailed understanding of the mechanisms that are clinically relevant in leukemia might help to predict and overcome drug resistance, thereby improving chemotherapy and the outcomes of cancer patients.

Autophagy is a general term for processes by which cytoplasmic material including organelles reach lysosomes for degradation [7,8]. It has a critical role in survival under stress conditions, whereas it also contributes to cell death when overactivated [9]. Recent reports demonstrate that ER may be a major source of or scaffold for the autophagic isolation membrane [10,11]. Disruption of homeostasis may lead to accumulation of misfolded or unfolded proteins in the ER lumen, a condition known as ER stress. The unfolded protein response (UPR), the major ER stress pathway, is a potent stimulator of autophagy [12]. According to Rouschop's study, activated PERK could inhibit the translation of proteins in the ER through inactivation of initiation factor eIF2α, which mediates the transcriptional activation of autophagy-related proteins LC3 and Atg5 during hypoxic response through action of ATF4 and CHOP, respectively [13]. ATF4 is a transcription factor that is responsible for expression of UPR genes, such as *chop/gadd153* and *gadd34*, which function in amino acid and redox metabolism [14]. Besides, accumulating evidences implied essential roles of some kinases in autophagy-integrated stress response [15]. p38MAPK, which belongs to a class of mitogen-activated protein kinases (MAPK), participates in a signaling cascade that controls the cellular responses to cytokines and stress.

Additionally, there have been conflicting reports showing that p38MAPK can either mediate cell survival through autophagy or cell death through apoptosis [16–18], suggesting the importance

* Corresponding author. Address: Department of Biochemistry and Molecular Biology, Institute of Basic Medical Sciences, CAMS & PUMC, 5 DongdanSantiao, Dongcheng District, Beijing 100005, China. Fax: +86 10 65296445.
E-mail addresses: sunriseday72@163.com, cmxu@ibms.pumc.edu.cn (C. Xu).

0014-5793/$36.00
http://dx.doi.org/10.1016/j.febslet.2013.06.011

of understanding p38MAPK functions under certain conditions. Therefore, the aim of this study was to determine whether p38MAPK contributes to signaling balance between apoptosis and autophagy in T-ALL-derived Jurkat cells, and to determine how the mediation of p38MAPK for directing the cell toward an ultimate fate of either autophagy or apoptosis.

2. Materials and methods

2.1. Cell models

The human T-acute lymphoblastic leukemia (T-ALL) Jurkat cells were cultured in RPMI 1640 medium (Gibco, Invitrogen) with 10% FCS, 100 units/ml penicillin, and 100 μg/ml streptomycin at 37 °C in a humidified incubator containing 5% CO_2. Plasmids pCMV5-Flag-p38MAPKα (dominant negative) was purchased from Addgene. siRNA against p38MAPK, eIF4E, MKK6, Mnk1 and non-silencing scrambled siRNA were synthesized by GenePharma (see Supplementary Table 1 for the sequences). The cells were transfected with 5–10 μg of plasmid DNA or 100 nM siRNA using Lipofectamine 2000 (Invitrogen Life Technologies, CA, USA) or RNAiMAX (Invitrogen), respectively. The transfected cells were used for the subsequent experiments after 24 h.

2.2. Reagents and antibodies

Sodium selenite (#S5261), 3-Methyladenine (#M9281), Bafilomycin A1 (#B1793), anti-β-actin (#A2228) and anti-GST (#G7781) were purchased from Sigma–Aldrich. The chemical inhibitors SB203580 (#559389), PD98059 (#513000), SP600125 (#420119), and Mnk1 inhibitor (#CGP57380) were from Merck. The antibody against Hsp90 (#SPA-843) used for western blotting was purchased from Stressgen Biotechnologies; the antibody against Hsp90 (#BM1587) used for co-immunoprecipitation was purchased from Boster Biological Technology (Wuhan, China). The antibody against p62 (#ab56416) was purchased from Abcam. Anti-PERK (#3179), -eIF2α (#9722), -p-eIF2α (#9721), -p-p38MAPK (# 9211), -MAPKAPK2 (#3042), -p-MAPKAPK2 (#3007), -p-MKK3/6 (#9236), -MKK6 (#9264), -p-eIF4E (#9741), -eIF4E (#2067), -Mnk1 (#2195), -cleaved caspase-3 (#9661), -cleaved PARP (#9546), -LC3B (#2775), -Beclin1 (#3738), -DYKDDDDK-Tag (#2369) and -GFP (#2555) antibodies were purchased from Cell Signaling Technology. Anti-ATF4 (#sc-200), -CHOP (#sc-793), -p-PERK (#sc-32577), p38MAPK (#sc-7972), -MEK3/6 (#sc-136982)and -B23 (#sc-32256) antibodies were from Santa Cruz Biotechnology.

2.3. Real-time PCR analyses

Total RNA was isolated using the Trizol reagent (Invitrogen, #15596) as described previously [6]. Reverse transcription was performed using the M-MLV Reverse Transcriptase (Promega, #M1701). 2 μl of a 1:10 dilution of the synthesized cDNA were used for quantitative real-time PCR. Real-time PCR was performed using SyberGreen PCR MasterMix (Applied Biosystems) on the 7500 RT-PCR system (Applied Biosystems). Relative mRNA levels were determined by comparing threshold cycles of amplified genes with GAPDH using the ΔCT method. Sequences for PCR primers are described in Supplementary Table 2.

2.4. Flow-cytometric analysis for apoptosis

The apoptosis detection was performed according to the manual of the Annexin-V-FITC apoptosis detection kit as previously described.

2.5. Growth inhibition assay

The cells were seeded at a density of 2×10^3 per well after treatment with the indicated chemicals. The cell counting kit-8 (CCK8) assay was performed according to the instructions of the manufacturer (Dojindo, Japan). The absorbance of each sample was analyzed using a Synergy H4 Hybrid Microplate Reader (Bio-Tek, USA) at 450 nm, with 620 nm as the reference wavelength.

2.6. Transmission electron microscopy

The cultured cells were fixed in 2.5% glutaraldehyde for 1 h, postfixed in 1% osmium tetroxide for 1 h at 48 °C and processed for embedding in the culture dish. The cells were then gently scraped and embedded in blocks of epon araldite. Thin sections were stained with 4% aqueous uranyl acetate and lead citrate and examined using a JEOL transmission electron microscope.

2.7. Preparation of subcellular fractions, co-immunoprecipitation and immunoblotting

The subcellular fractions for the immunoprecipitation assay and immunoblotting were prepared as previously described [6]. After measuring the protein concentrations (Bradford Method), the proteins were detected by western blotting with the indicated antibodies. Each result represents three independent experiments.

2.8. GST pull-down assays

GST-tagged MAPK14 (p38 alpha) inactive fusion protein was purchased from Invitrogen. Cell lysates were incubated overnight with 5 μg of GST-tagged p38 fusion protein and then 30 μl of glutathione-agarose beads (Sigma–Aldrich) for 3 h at 4 °C with end-over-end mixing. After thorough washing, the bound proteins were separated by SDS–PAGE and detected by western blotting using the appropriate antibodies.

2.9. Immunofluorescence

The protocol for immunostaining the cells was described previously [6]. Briefly, the cells were fixed, permeabilized, and incubated with primary antibodies, washed in PBS and incubated with FITC- or CY3-conjugated secondary antibodies (Jackson ImmunoResearch). The cells were stained with 1 μM DAPI (Sigma–Aldrich) for 5 min. Images were captured using a Zeiss Axioscope microscope.

2.10. Chromatin immunoprecipitation assay

ChIP was performed using the SimpleChIP Enzymatic Chromatin IP Kit (Cell Signaling Technology) as described previously [6]. For precipitation, the anti-ATF4 antibody (CREB [C-20], Santa Cruz Biotechnologies Inc.) was used. Following extensive washing, the bound DNA fragments were eluted and analyzed by PCR using primers specific for the *map1lc3b* and *chop* promoters (see Supplementary Table 3 for primers). Real-time PCR was performed using the SuperArray PCR master mix and iCycle iQ5 Multicolor Detection System (Bio-Rad) according to the manufacturer's instructions; the results were normalized to the chromatin input of the IP.

2.11. Statistical analysis

The values are presented as the means ± S.E.M., and the statistical analysis was performed using ANOVA, followed by a multiple comparison test for the multiple experimental groups. In some

cases, Student's *t*-test was used for comparing two of the groups. Differences were statistically significant at $P < 0.05$.

3. Results

3.1. Selenite induces ER stress-mediated cell apoptosis, and p38MAPK is responsible for the up-regulation of ATF4 in Jurkat cells

Previous results suggested that sodium selenite possessed anti-tumor effect by inducing cell apoptosis and autophagy. We therefore performed FACS and western blot to determine the effect of selenite on ER-stress. Fig. 1A shows increases in cell apoptotic rate from FACS assay demonstrated typical apoptosis induced by 20 μM selenite. Moreover, phosphorylation of PERK and eIF2α appeared at 6 h and 9 h, but was not sustained for up to 24 h, possibly due to the short duration of activation of PERK. The induction of ATF4 by selenite gradually increased regardless of the phosphorylation status of eIF2α. The expression of CHOP, a transcriptional regulator involved in apoptosis, increased after 6 h, peaked at 12–15 h and declined to a low level at 24 h (Fig. 1A, lower panel). In addition, the ER stress inducer tunicamycin (Tm), which inhibits *N* glycosylation, was used as a positive control. Immunoblotting and FACS results showed in Fig. 1B confirmed activation of typical PERK/eIF2α/ATF4 UPR pathway by Tm during cell apoptosis. Also, we detected change in the cellular distribution of ATF4, and immunoblotting results revealed that the expression of ATF4 increased in both nuclear and cytoplasmic fractions (Fig. 1C).We therefore hypothesized that a different apoptosis-response was induced, at least in part, through differential activating the transcription factor ATF4 and CHOP.

As MAPK has known roles in various stress signal transduction pathways, the MAPK inhibitors SB203580 (p38MAPK), PD98059 (ERK), and SP600125 (JNK) were combined with selenite to examine the ATF4 expression. We observed that the addition of SB203580 to the Jurkat cell cultures in the presence of selenite strongly abrogated the up-regulation of ATF4 (Fig. 1D), but the other inhibitors had no effect on ATF4 expression (data not shown), suggesting the involvement of p38MAPK in ER stress-related cell apoptosis. Fig. 1E showed the induction of p38MAPK activity by selenite occurs in time- and dose-dependent manners in Jurkat

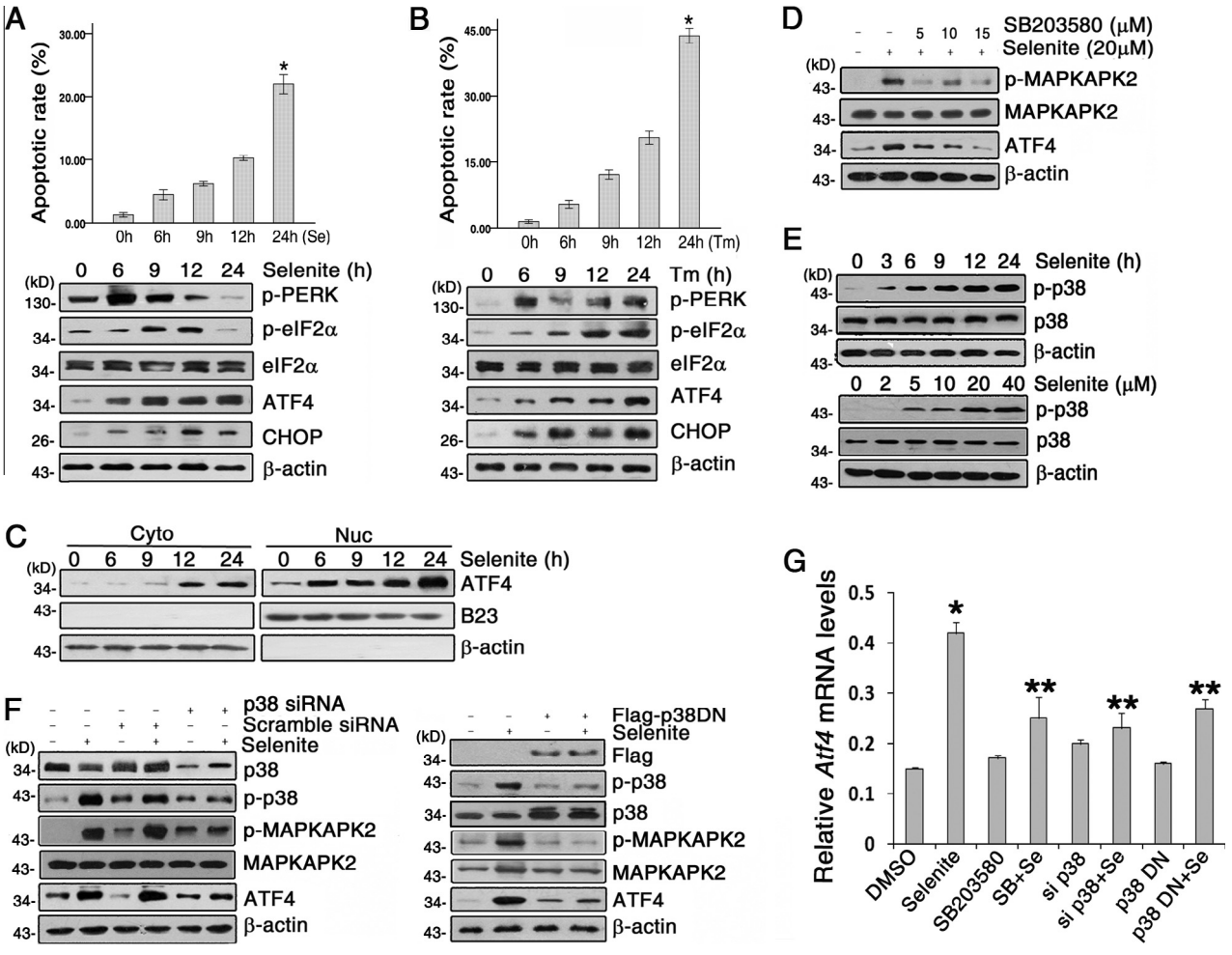

Fig. 1. p38MAPK up-regulates the expression of ATF4 in response to selenite-induced ER Stress. (A and B) Jurkat cells were treated with 20 μM sodium selenite (A) or 0.1 μg/ml tunicamycin (B) for the indicated times. The apoptotic rate of cells was determined by FACS (upper panels). Protein extracts were subjected to western blotting to detect p-PERK, p-eIF2α, eIF2α, ATF4 and CHOP (lower panels). (C) Cells were exposed to selenite for the indicated times, cytoplasmic and nuclear fractions were extracted, and ATF4 was detected by western blotting. The purity of the cytoplasmic and nuclear proteins was confirmed using β-actin and B23, respectively. (D) Cells were pretreated with different concentrations of SB203580 prior to selenite treatment for 24 h, after which time p-MAPKAPK2, MAPKAPK2, ATF4 were analyzed via western blot. (E) Cells were exposed to selenite for different durations or at different concentrations and the p-p38MAPK and p38MAPK expression levels were then analyzed. (F) Cells were transfected with p38MAPK-siRNA (left panel) or plasmid-p38DN (right panel) before selenite exposure for 24 h, and then p-p38MAPK, p38MAPK, ATF4 and Flag were detected by western blotting. (G) *Atf4* mRNA levels were quantified by real-time RT-PCR after cells were treated as described in (D and F). The data are presented as the means ± S.D. ($n = 3$). $^{*}P < 0.01$ compared with the control group. $^{**}P < 0.05$ compared with the selenite-treated group.

cells. For further confirmation, cells were transfected with p38MAPK-siRNA or a dominant-negative p38MAPK plasmid (plasmid-p38DN) to reduce endogenous expression or activity of p38MAPK, respectively. The inhibition efficiency was confirmed by detecting p-MAPKAPK2 levels, which is the substrate of p38MAPK. Also, statistical analysis of p-MAPKAPK2/MAPKAPK2 ratio was conducted and showed in Fig. S1. As expected, the expression of both ATF4 protein and *Atf4* mRNA levels were reduced to basal levels compared to the selenite-alone treatment group (Fig. 1F and G). Collectively, p38MAPK is possibly involved in the selenite-induced ER stress in Jurkat cells.

3.2. p38MAPK activity is required for selenite-induced apoptosis and autophagy in Jurkat cells

To investigate the role of p38MAPK in apoptosis and autophagy, we employed CCK8 assay and the results showed that inhibition of p38MAPK improved cell survival rates (Fig. 2A). In addition, silencing p38MAPK decrease apoptosis significantly proved by FACS assay, which indicates that p38MAPK is an important mediator of the apoptotic response to selenite (Fig. 2B). In a previous report, we provided preliminary evidence that selenite triggers autophagy during apoptosis in Jurkat cells [6]. Therefore, we further investigated the participation of p38MAPK in this process. Fluorescent microscopy of GFP-LC3 transient transfection experiments was firstly performed to visualize autophagy. The redistribution of LC3 from discrete vesicular structures (punctate fluorescence) to a diffuse cytoplasmic localization and the conversion of LC3II protein to LC3I protein proved the reduced levels of autophagy when p38MAPK was blocked (Fig. 2C and D). Fig. 2E illustrates ultrastructural studies using transmission electron microscopy (TEM), which reveal scattered double-membrane structures containing recognizable cellular organelles in selenite-treated Jurkat cells. However, induction of autophagy by selenite was suppressed when p38MAPK was inhibited or depleted. Three biochemical markers of autophagy, namely p62, Beclin1 and LC3I/II, were detected. As shown in Fig. 2F, activity inhibition or expression depletion of p38MAPK led to both accumulation of p62 and downregulation of Beclin1 and LC3II, which suggested essential roles of p38MAPK in selenite-induced autophagy. We further assessed the effect of p38MAPK on selenite-elicited apoptosis, and found that the cleavage of caspase3 and PARP by selenite were significantly blocked when p38MAPK was inhibited in Jurkat cells (Fig. 2F), indicating that p38MAPK activation is required for selenite-induced autophagy and cell death.

3.3. ATF4 binds to the map1lc3b and chop promoters

To elucidate the role of ATF4 expression in apoptosis and autophagy induction, and considering our previous results, we next investigated the connection between ATF4 and gene transcription in response to selenite. The ATF/CREB family consists of transcription factors that function by binding to the cAMP-responsive element (CRE) palindromic octanucleotide TGACCTCA [19]. An analysis of the *map1lc3b* promoter revealed the existence of two CRE-like elements at nt -528(a site) and nt -1895 (A site); the elements were also found in the promoter of the known ATF4 target gene *chop* (b site and B site) (Fig. 3A). Subsequent ChIP assays confirmed an enrichment of ATF4 on both the *map1lc3b* and *chop* promoters (Fig. 3B, the primary data shown in Fig. S2). Moreover, it is noteworthy that the amount of enriched ATF4 on the *map1lc3b* promoter increased following the addition of selenite to Jurkat cells, whereas SB203580 co-treatment markedly inhibited the enrichment because of the inhibition of p38MAPK activity. Simultaneously, we observed the expression of *chop* mRNA levels were reduced to basal levels compared to the selenite-alone treatment group (Fig. 3C). In order to ascertain these findings, we performed western blot analysis to examine the expression of the two ATF4-targeted proteins, LC3I/II and CHOP, in SB203580-pretreated, p38 siRNA- or plasmid-p38DN-transfected cells. Immunoblotting results showed that changes in CHOP and LC3I/LC3II protein levels were consistent with gene expression. Moreover, the decreases in LC3II/LC3I ratio were detected in p38MAPK-inhibition groups compared to selenite-only treatment groups, suggesting an important effect of ATF4 on controlling autophagy (Fig. 3D–F). Therefore, the provided experimental evidence suggests that ATF4 balances cellular processes, at least in part, by favoring the expression of both *map1lc3b*, which plays a role in autophagy, and *chop*, which plays a role in apoptosis, in Jurkat cells.

3.4. p38MAPK co-localized with MKK3/6 in Jurkat cells in response to selenite

It has been shown that p38MAPK activity is regulated by multisite phosphorylation through various protein kinases, including MAPK kinase (MKK) 3 and MKK6 [20]. Therefore, we initially detected the effect of selenite on MKK3/6 activation. Fig. 4A shows the phosphorylation of MKK3/6 in Jurkat cells treated with selenite for various times and concentrations, implying a typical cascade activation induced by selenite. Additionally, p38MAPK can also be activated independently of MKK3/6 via autophosphorylation [21]. According to recent report that the dissociation of the p38MAPK-Hsp90 complex is a key step in the autophosphorylation of p38MAPK, we next examined whether the activation of p38MAPK in Jurkat cells was correlated with Hsp90. Co-immunoprecipitation showed only the cellular interaction between MKK3/6 and p38MAPK in Jurkat cells, but no direct association between Hsp90 and p38MAPK was observed (Fig. 4B). Additionally, we conducted a GST pull-down assay using the purified GST-tagged p38MAPK protein to pull down endogenous Hsp90 or MKK3/6 and confirmed these findings in vitro (Fig. 4C). To provide convincing evidence, direct experiments were performed and the results showed that RNAi targeting for MKK6 decreased the phosphorylation of both MKK3/6 and p38MAPK (Fig. 4D), which suggested the activity of p38MAPK was modulated at least in part through activating MKK3/6. Immunofluorescence microscopy results also revealed that endogenous p38MAPK was localized to MKK3/6 but not Hsp90 in selenite-treated Jurkat cells (Fig. S3). These results together indicated that MKK3/6 functions as an important upstream regulator of p38MAPK in this process.

3.5. The promoter selectivity of ATF4 depends on p38MAPK-phosphorylated eIF4E

As we found the phosphorylation of eIF2α persisted for a shorter period of time in response to selenite, which did not quadrate with the continuous ATF4 upregulation, we examined the effects of selenite on eIF4E, another upstream regulator of ATF4 [22]. Compared with control files, the eIF4E in Jurkat cells was gradually phosphorylated at S209 and accompanied by unchanged total eIF4E levels with time under selenite exposure conditions (Fig. 5A). Moreover, we found that the changes of p-eIF4E in both cytoplasmic and nuclear extracts were consistent with the whole cell lysates (Fig. 5B). Since Mnk1/2 kinases have been reported to target eIF4E S209 site [23], we examined involvement of eIF4E in the promoter selectivity of ATF4 using Mnk1 inhibitor and eIF4E-specific siRNA. Immunoblotting results showed that Mnk1 inhibitor profoundly suppressed eIF4E phosphorylation without affecting total eIF4E levels. Notably, we found that either chemical inhibitor or expression of eIF4E-RNAi in Jurkat cells significantly blocked the upregulation of ATF4 under selenite exposure conditions (Fig. 5C). To further ascertain these findings, we performed

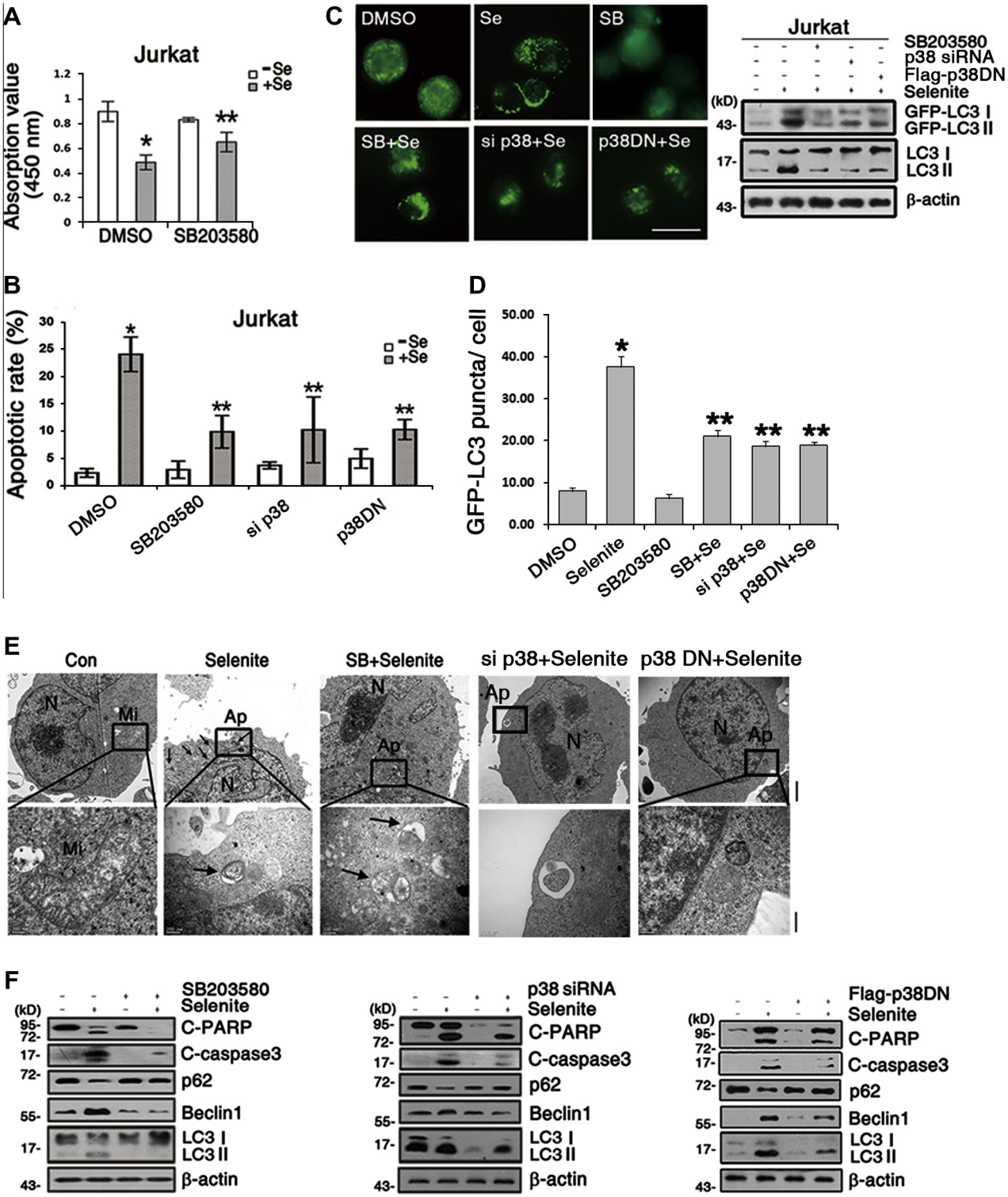

Fig. 2. Effect of p38MAPK on apoptosis and autophagy during selenite exposure in Jurkat cells. (A) Cells were pretreated with 10 μM SB203580 for 1.5 h before selenite treatment for 24 h, and cell viability was analyzed by CCK8 assay. (B) The effect of p38MAPK inhibition, depletion or dominant-negative plasmid transfection on the selenite-induced apoptosis in Jurkat cells was analyzed by Annexin-V assay. (C) Punctate GFP-LC3 fluorescence in GFP-LC3-transfected cells treated with selenite in the presence or absence of SB203580, p38MAPK-siRNA or the plasmid-p38DN (left panel). Scale bar: 20 μm. The expression of GFP-LC3-I and -II in GFP-LC3-transfected cells treated with the indicated reagents using anti-GFP and anti-LC3 antibodies (right panel). (D) The average number of GFP-LC3 puncta per cell. Each data point represents a total of 30 cells from four independent experiments for each protocol. (E) Electron micrograph of Jurkat cells pre-incubated with or without 10 μM SB203580 for 1.5 h or transfected with p38-siRNA or the plasmid-p38DN before selenite treatment. Black arrows indicate the autophagosomes. Scale bar: 1 μm (upper panels); 0.2 μm (bottom panels). N, nucleus; Mi, mitochondria; Ap, autophagosomes. (F) Cells were pretreated with 10 μM SB203580 for 1.5 h or transfected with p38-siRNA or the plasmid-p38DN before selenite treatment, then C-PARP, C-caspase3, p62, Beclin1 and LC3I/II levels were determined by western blot and normalized with β-actin. Data are presented as means ± SD ($n = 3$). $^{*}P < 0.01$ compared with the control group. $^{**}P < 0.05$ compared with the selenite treatment group.

a ChIP assay and observed less binding of ATF4 to both *map1lc3b* and *chop* promoters when the expression or activity of eIF4E was inhibited, compared with selenite-treatment group (Fig. 5D, the primary data shown in Fig. S4). To determine whether eIF4E-mediated transcriptional activity of ATF4 is dependent on p38MAPK, we verified that the p38MAPK activation was essential to phosphorylate eIF4E (Fig. 5E). To assess whether autophagy levels was affected by eIF4E directly, fluorescent microscopy of GFP-transfection cells was performed and the results of fluorescence punctate distribution were in agreement with those provided by

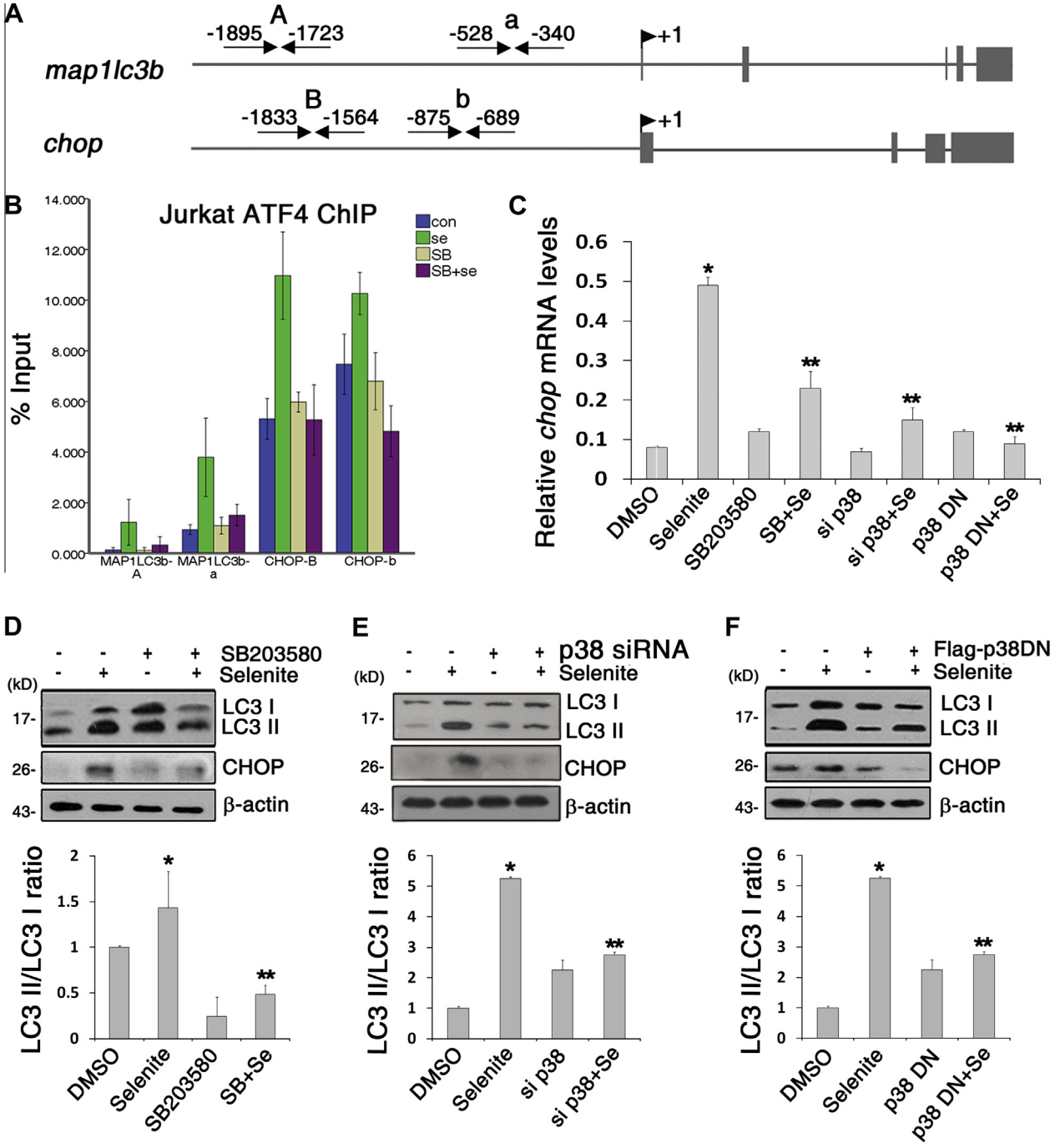

Fig. 3. ATF4 was directly involved in *map1lc3b* and *chop* transcription in response to selenite treatment. (A) A schematic diagram showing the location of the primer pairs used for the quantitative PCR (qPCR) analysis following ChIP. (A) (a) two putative ATF4 binding CRE sites on *map1lc3b*; (B) (b) two putative ATF4 binding CRE sites on *chop*. (B) Quantitative ChIP analysis of ATF4 occupancy on the *map1lc3b* and *chop* genes under the indicated conditions was performed by qPCR. The ChIP assay performed using an anti-ATF4 antibody was compared with normal rabbit IgG as a negative control. The data are expressed as the percentage of input DNA and represent the means ± SD ($n = 3$). (C) *chop* mRNA levels were quantified by real-time RT-PCR after cells were treated with selenite in the presence or absence of 10 μM SB203580, p38MAPK-siRNA or the plasmid-p38DN. (D–F) Cells were treated with selenite for 24 h in the absence or presence of 10 μM SB203580 and/or the plasmid-p38DN. Western blot assay was performed to detect LC3I/II and CHOP protein expression levels (upper panels). The ratio of LC3II/LC3I was calculated to reflect the conversion of LC3I to LC3II (lower panels). Data were presented as means ± SD ($n = 3$) and expressed as the percentage of the control. $^{*}P < 0.01$ compared with the control group. $^{**}P < 0.05$ compared with the selenite treatment group.

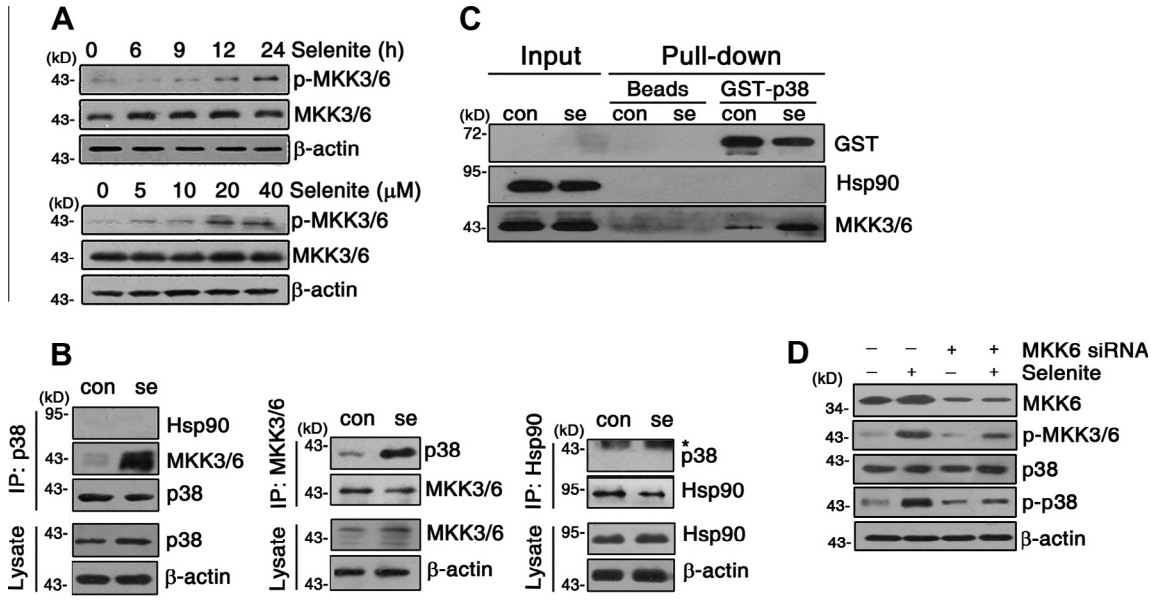

Fig. 4. Selenite promotes the interaction between p38 and MKK3/6 in Jurkat cells. (A) Jurkat cells were exposed to selenite for different times (upper panel) or at different concentrations (lower panel), and the expression of p-MKK3/6 and MKK3/6 was analyzed via immunoblotting. (B) Protein extracts prepared from cells were immunoprecipitated with specific antibodies against p38MAPK, Hsp90 or MKK3/6. The immune complexes and the 10% input were analyzed using the indicated antibodies. IP, immunoprecipitation; IB, immunoblotting; *, the immunoglobulin heavy chain. (C) Cells were lysed after 24 h of treatment and subjected to a GST pull-down assay. Precipitates and total cell lysates were analyzed by immunoblotting and probed with the indicated antibodies to detect the co-precipitated proteins. (D) Cells were transient transfected with MKK6-specific siRNA before selenite was added, and then p38MAPK and p-p38MAPK levels were detected via immunoblotting.

ChIP assay (Fig. 5F). Taken together, our data demonstrate the importance of eIF4E to the selenite-induced apoptosis and autophagy in Jurkat cells.

3.6. Autophagy induction enhances selenite-induced cell apoptosis

Recent findings demonstrated the crosstalk between apoptotic and autophagic signaling pathways. To elucidate the complex interplay and characterize the autophagic flux in this process, we firstly used two pharmacological inhibitors of autophagy, 3-Methyladenine (3-MA, 10 mM) and Bafilomycin A1 (Baf A1, 100 nM), to specifically inhibit the basal levels of autophagy in Jurkat cells. Both the punctate GFP-LC3 fluorescence and western blot analysis in Fig. 6A–C confirmed the inhibitory efficiency. To further investigate the role of p38MAPK in the conversation between apoptosis and autophagy, we treated cells with selenite for 24 h in the absence or presence of 3-MA or SB203580 or both of them for 1.5 h, and then examined the cleavage of apoptotic-related protein and cell apoptotic rate by western blot and Annexin-V assay, respectively. These results showed that 3-MA markedly protected cells from selenite-elicited apoptosis. Moreover, the protective effects increased when SB203580 was added before 3-MA and selenite (Figs. 6D and S5). These results indicated that p38MAPK-modulated autophagy intensified apoptotic effect, which ultimately accelerated cell demise.

4. Discussion

Similar to other cancers, the major obstacles for leukemia chemotherapy are the cytoxicity of the anticancer agents in normal cells and drug resistance of tumor cells. In the past few years, we have demonstrated statistically significant antitumor effect of selenite, without any adverse effects both in vitro and in vivo [6,24–26]. Additionally, selenite moderates metastatic progression of tumor cells to liver, suggesting the potential clinical application of selenite in leukemia therapy. Understanding the mechanisms involved in regulation of apoptosis and autophagy and their interplay becomes a central question in controlling cell growth and leukemic transformation [27–29]. In this study, we found that MKK3/6/p38MAPK/eIF4E cascades is involved in the induction of apoptosis and autophagy that is achieved through upregulating a transcriptional factor ATF4, which are schematically summarized in Fig. 7.

Studies over the past decade have linked the PERK/eIF2α/ATF4 UPR branch to ER stress-related autophagy via phosphorylated eIF2α-triggered conversion of LC3 in various diseases, including Huntington's disease and Parkinson's disease [14,30]. Recently, Rouschop et al. demonstrated that ATF4 and CHOP, which are substrates of eIF2α, increased the transcription of essential autophagy genes under hypoxia [13,31], supporting involvement of UPR in autophagy. In accord with that, we determined the binding of ATF4 at CRE-like elements in the *map1lc3b* promoter [13,31,32], which is involved in formation of autophagosomal vacuoles, a hallmark of autophagy. Interestingly, we observed a transient activation of the PERK/eIF2α pathway during Jurkat cells exposed to selenite, indicating a chronic ER stress was induced to lead to cellular adaption. Therefore, the sustained upregulation of ATF4 suggested other pathway functioned in this process.

To date, there is abundant evidence for involvement of p38MAPK in apoptosis and autophagy. Wang et al. have reported that protective action of selenite on ischemia renal injury was associated with reducing activation of ASK1/MKK3/p38 signal pathway [33], implying that p38MAPK cascades lead to excessive cell apoptosis in kidney, which was consistent with ours on this point. However, here we proved reverse effects of selenite on our experimental model, which may be due to complex cellular and molecular mechanisms. Meanwhile, p38MAPK can be considered as either an inducer or an inhibitor of autophagy depending on the stimulus. For instance, it has been described that the abrogation of p38 by SB203580 is sufficient to interfere with normal autophagic maturation steps [34]. Also, Keil et al. proved that the regulation of p38 by Gadd45β/MEKK4 negatively regulates auto-

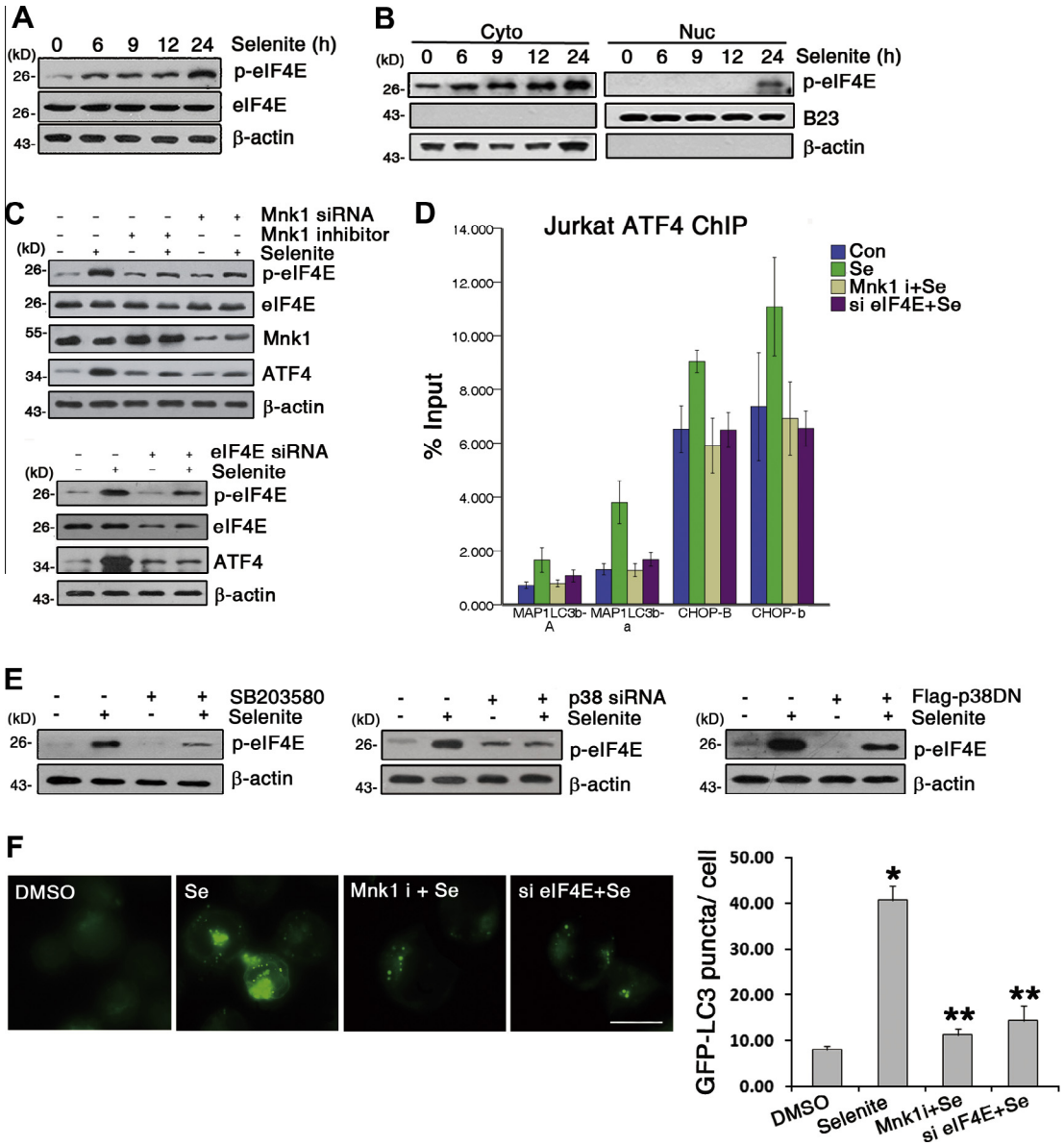

Fig. 5. p38MAPK-phosphorylated eIF4E is responsible for the binding of ATF4 on *chop* and *map1lc3b*. (A and B) Cells were exposed to selenite for the indicated times and the p-eIF4E and eIF4E expression levels were examined in the whole cell lysate (A) or the cytoplasmic and nuclear fractions (B) by immunoblotting. The purity of the cytoplasmic and nuclear proteins was confirmed using β-actin and B23, respectively. (C) Western blots of p-eIF4E, eIF4E and ATF4 after cells were co-treated with Mnk1 inhibitor (1 μM) (upper panel) or transfected with eIF4E-siRNA (lower panel) before selenite treatment. (D) Quantitative ChIP analysis of ATF4 occupancy on the *map1lc3b* and *chop* genes under the indicated conditions was performed by qPCR. Data are expressed as the percentage of input DNA and represent the means ± SD ($n = 3$). (E) Cells were pretreated with 10 μM SB203580 or transfected with p38-siRNA or p38-DN plasmid before selenite exposed for 24 h, and then p-eIF4E levels were determined using immunoblotting. (F) Punctate GFP-LC3 fluorescence in GFP-LC3-transfected cells treated with selenite in the presence or absence of Mnk1 inhibitor or eIF4E-siRNA. Right panel: Representative images (scale bar: 20 μm); Left panel: The average number of GFP-LC3 puncta per cell. Each data point represents a total of 30 cells from five independent experiments for each protocol, means ± SD. $^{*}P < 0.01$ compared with the control group. $^{**}P < 0.05$ compared with the selenite treatment group.

phagic process [35]. According to immunoprecipitation and immunofluorescence assays, we proved that the canonical MKK3/6 axis was required for p38MAPK activation in Jurkat cells, and blockage of p38MAPK provoked a marked decrease in autophagy in response to selenite, suggesting a dual role of p38MAPK in selenite-elicited apoptosis and autophagy. It's coincident with our previous assumption.

One of the protein translational controllers, eIF4E, plays a critical role in cap-dependent translation initiation, and various upstream modulators of eIF4E, such as AKT/mammalian target of rapamycin (mTOR), MEK/ERK, and p38MAPK/MAP kinase-interacting kinase-1 (MNK1), have been identified [22,36,37]. It's interesting in our data that during selenite treatment, eIF4E was phosphorylated at site S209 through the p38MAPK activity in Jurkat cells, even though a direct association between p38MAPK and eIF4E was not observed. Based on our data (Fig. 5) we proposed that the MKK3/6-dependent activation of p38MAPK in Jurkat cells somehow transduced the signal to eIF4E, thus eIF4E-dependent translation of ATF4 appeared to facilitate binding to both the *chop* and *map1lc3b* promoters in response to selenite. The detailed signaling pathway for the translation of ATF4 regulated by eIF4E awaits further analysis.

As a complementary mechanism of apoptosis, autophagy is often referred to either pro-death or pro-survival strategy according to certain conditions. The results of the present study showed a reduction of apoptotic rate in cells pre-treated with autophagy

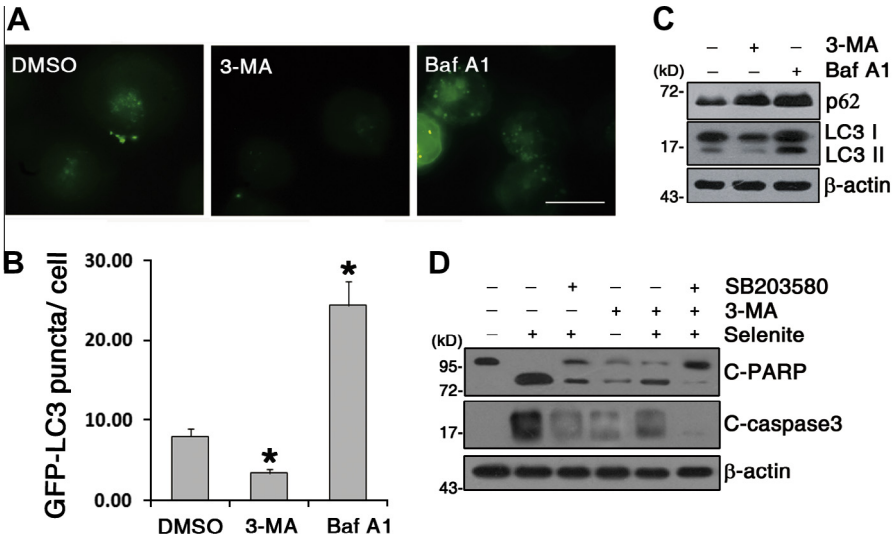

Fig. 6. Inhibition of autophagy attenuated selenite-induced cell apoptosis. (A) Representative images of punctate GFP-LC3 fluorescence in GFP-LC3-transfected cells treated with selenite in the presence or absence of 3-MA (10 mM) or Baf A1 (100 nM) for 1.5 h. Bar, 20 μm. (B) The average number of GFP-LC3 puncta per cell. Each data point represents a total of 30 cells from five independent experiments for each protocol, means ± SD. *$P < 0.01$ compared with the control group. (C) Western blot analysis of p62 and LC3I/II in cells treated as described in (A). (D) Cells were incubated with SB203580 (10 μM) or 3-MA, or both of them for 1.5 h before selenite treatment for 24 h, as described in the text, and then C-PARP and C-caspase3 levels were determined by immunoblotting and normalized with β-actin.

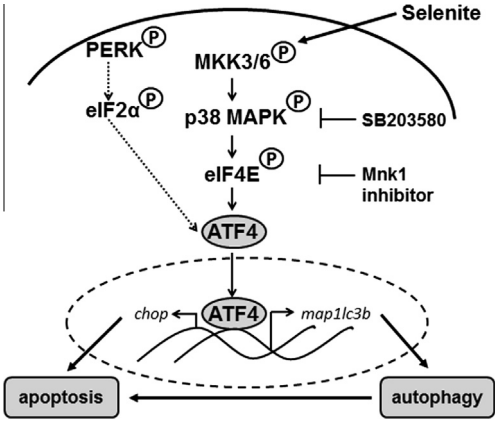

Fig. 7. Activation of MKK3/6/p38MAPK/eIF4E axis led to cell demise in selenite-treated Jurkat cells. Schematic model depicting the involvement of MKK3/6/p38MAPK/eIF4E selenite-responsive, ATF4-mediated apoptosis and autophagy regulation. Upon selenite treatment, the MKK3/6/p38MAPK signaling pathways converge at ATF4 to regulate *map1lc3b* and *chop* transcription, with p-eIF4E playing essential role in apoptosis and autophagy induction. See the text for the detailed discussion on the roles of these signaling pathways and their interplay.

inhibitors, suggesting that autophagic cell death was induced by selenite. This information is extremely important because it supported our previous conclusions that selenite elicits transient adaption in the early stage through chronic ER stress, after which autophagy is immediately induced in concurrence with apoptosis and promotes irreversible cell demise.

Conflict of interest

The authors declare no conflicts of interest.

Acknowledgements

This work was supported by Grants from the National Natural Sciences Foundation of China (No. 3117088 and No. 30970655), the National Natural Science Foundation for Young Scholars of China (No. 31101018), the Natural Science Foundation of Beijing (No. 5082015), the State Key Laboratory Special Fund (No. 2060204) and the Ministry of Education, China for Doctor-training Unite (No. 20091106110025).

Appendix A. Supplementary data

Supplementary data associated with this article can be found, in the online version, at http://dx.doi.org/10.1016/j.febslet.2013.06.011.

References

[1] Grossmann, V. et al. (2013) The molecular profile of adult T-cell acute lymphoblastic leukemia: mutations in RUNX1 and DNMT3A are associated with poor prognosis in T-ALL. Genes Chromosom. Cancer 52, 410–422.
[2] De Keersmaecker, K. et al. (2013) Exome sequencing identifies mutation in CNOT3 and ribosomal genes RPL5 and RPL10 in T-cell acute lymphoblastic leukemia. Nat. Genet. 45, 186–190.
[3] Park, E. et al. (2011) Targeting survivin overcomes drug resistance in acute lymphoblastic leukemia. Blood 118, 2191–2199.
[4] Pillozzi, S. et al. (2011) Chemotherapy resistance in acute lymphoblastic leukemia requires hERG1 channels and is overcome by hERG1 blockers. Blood 117, 902–914.
[5] Guan, L., Han, B., Li, Z., Hua, F., Huang, F., Wei, W., Yang, Y. and Xu, C. (2009) Sodium selenite induces apoptosis by ROS-mediated endoplasmic reticulum stress and mitochondrial dysfunction in human acute promyelocytic leukemia NB4 cells. Apoptosis 14, 218–225.
[6] Jiang, Q. et al. (2011) Heat shock protein 90-mediated inactivation of nuclear factor-kappaB switches autophagy to apoptosis through becn1 transcriptional inhibition in selenite-induced NB4 cells. Mol. Biol. Cell 22, 1167–1180.
[7] Levine, B. and Kroemer, G. (2008) Autophagy in the pathogenesis of disease. Cell 132, 27–42.
[8] Mizushima, N. and Komatsu, M. (2011) Autophagy: renovation of cells and tissues. Cell 147, 728–741.
[9] Behrends, C., Sowa, M.E., Gygi, S.P. and Harper, J.W. (2010) Network organization of the human autophagy system. Nature 466, 68–76.
[10] Salazar, M., Hernandez-Tiedra, S., Torres, S., Lorente, M., Guzman, M. and Velasco, G. (2011) Detecting autophagy in response to ER stress signals in cancer. Methods Enzymol. 489, 297–317.
[11] Hayashi-Nishino, M., Fujita, N., Noda, T., Yamaguchi, A., Yoshimori, T. and Yamamoto, A. (2009) A subdomain of the endoplasmic reticulum forms a cradle for autophagosome formation. Nat. Cell Biol. 11, 1433–1437.
[12] Kroemer, G., Marino, G. and Levine, B. (2010) Autophagy and the integrated stress response. Mol. Cell 40, 280–293.
[13] Rouschop, K.M. et al. (2010) The unfolded protein response protects human tumor cells during hypoxia through regulation of the autophagy genes MAP1LC3B and ATG5. J. Clin. Invest. 120, 127–141.

[14] Kouroku, Y. et al. (2007) ER stress (PERK/eIF2alpha phosphorylation) mediates the polyglutamine-induced LC3 conversion, an essential step for autophagy formation. Cell Death Differ. 14, 230–239.
[15] Webber, J.L. and Tooze, S.A. (2010) Coordinated regulation of autophagy by p38alpha MAPK through mAtg9 and p38IP. EMBO J. 29, 27–40.
[16] de la Cruz-Morcillo, M.A. et al. (2011) P38MAPK is a major determinant of the balance between apoptosis and autophagy triggered by 5-fluorouracil: implication in resistance. Oncogene 31, 1073–1085.
[17] Moruno-Manchon, J.F., Perez-Jimenez, E. and Knecht, E. (2013) Glucose induces autophagy under starvation conditions by a p38 MAPK-dependent pathway. Biochem. J. 449, 497–506.
[18] Zhan, Y., Gong, K., Chen, C., Wang, H. and Li, W. (2012) P38 MAP kinase functions as a switch in MS-275-induced reactive oxygen species-dependent autophagy and apoptosis in human colon cancer cells. Free Radic. Biol. Med. 53, 532–543.
[19] Koyanagi, S., Hamdan, A.M., Horiguchi, M., Kusunose, N., Okamoto, A., Matsunaga, N. and Ohdo, S. (2011) CAMP-response element (CRE)-mediated transcription by activating transcription factor-4 (ATF4) is essential for circadian expression of the Period2 gene. J. Biol. Chem. 286, 32416–32423.
[20] Chang, L. and Karin, M. (2001) Mammalian MAP kinase signalling cascades. Nature 410, 37–40.
[21] Ota, A., Zhang, J., Ping, P., Han, J. and Wang, Y. (2010) Specific regulation of noncanonical p38 activation by Hsp90-Cdc37 chaperone complex in cardiomyocyte. Circ. Res. 106, 1404–1412.
[22] Chen, Y.J., Tan, B.C., Cheng, Y.Y., Chen, J.S. and Lee, S.C. (2010) Differential regulation of CHOP translation by phosphorylated eIF4E under stress conditions. Nucleic Acids Res. 38, 764–777.
[23] Silva, R.L. and Wendel, H.G. (2008) MNK, EIF4E and targeting translation for therapy. Cell Cycle 7, 553–555.
[24] Li, Z., Shi, K., Guan, L., Cao, T., Jiang, Q., Yang, Y. and Xu, C. (2010) ROS leads to MnSOD upregulation through ERK2 translocation and p53 activation in selenite-induced apoptosis of NB4 cells. FEBS Lett. 584, 2291–2297.
[25] Guan, L., Han, B., Li, J., Li, Z., Huang, F., Yang, Y. and Xu, C. (2009) Exposure of human leukemia NB4 cells to increasing concentrations of selenite switches the signaling from pro-survival to pro-apoptosis. Ann. Hematol. 88, 733–742.
[26] Huang, F. et al. (2009) Selenite induces redox-dependent Bax activation and apoptosis in colorectal cancer cells. Free Radic. Biol. Med. 46, 1186–1196.
[27] Shi, Y.H. et al. (2011) Targeting autophagy enhances sorafenib lethality for hepatocellular carcinoma via ER stress-related apoptosis. Autophagy 7, 1159–1172.
[28] Notte, A., Leclere, L. and Michiels, C. (2011) Autophagy as a mediator of chemotherapy-induced cell death in cancer. Biochem. Pharmacol. 82, 427–434.
[29] Jia, W., Pua, H.H., Li, Q.J. and He, Y.W. (2011) Autophagy regulates endoplasmic reticulum homeostasis and calcium mobilization in T lymphocytes. J. Immunol. 186, 1564–1574.
[30] Cherra 3rd, S.J., Dagda, R.K. and Chu, C.T. (2010) Review: autophagy and neurodegeneration: survival at a cost? Neuropathol. Appl. Neurobiol. 36, 125–132.
[31] Rzymski, T. et al. (2010) Regulation of autophagy by ATF4 in response to severe hypoxia. Oncogene 29, 4424–4435.
[32] Milani, M., Rzymski, T., Mellor, H.R., Pike, L., Bottini, A., Generali, D. and Harris, A.L. (2009) The role of ATF4 stabilization and autophagy in resistance of breast cancer cells treated with Bortezomib. Cancer Res. 69, 4415–4423.
[33] Wang, Y., Ji, H.X., Zheng, J.N., Pei, D.S., Hu, S.Q. and Qiu, S.L. (2009) Protective effect of selenite on renal ischemia/reperfusion injury through inhibiting ASK1-MKK3-p38 signal pathway. Redox Rep. 14, 243–250.
[34] Corcelle, E. et al. (2007) Control of the autophagy maturation step by the MAPK ERK and p38: lessons from environmental carcinogens. Autophagy 3, 57–59.
[35] Keil, E. et al. (2013) Phosphorylation of Atg5 by the Gadd45beta-MEKK4-p38 pathway inhibits autophagy. Cell Death Differ. 20, 321–332.
[36] Shveygert, M., Kaiser, C., Bradrick, S.S. and Gromeier, M. (2010) Regulation of eukaryotic initiation factor 4E (eIF4E) phosphorylation by mitogen-activated protein kinase occurs through modulation of Mnk1–eIF4G interaction. Mol. Cell. Biol. 30, 5160–5167.
[37] Nyfeler, B. et al. (2011) Relieving autophagy and 4EBP1 from rapamycin resistance. Mol. Cell. Biol. 31, 2867–2876.